A Review of Uncertainty Quantification of Estimation of Frequency Response Functions

Christopher Majba, Dr. Randall Allemang, Dr. Allyn Phillips
University of Cincinnati
School of Dynamic Systems, College of Engineering
2600 Clifton Avenue
Cincinnati, OH 45221-0072

Abstract
This paper will investigate methods for calculating the statistical reduction of variance in FRF measurements. Traditional analyses will be presented and the links to the analysis presented herein will be established. As the method for determining the variance, or confidence bounds, has changed since its first introduction nearly 40 years ago, both the original and more modern analysis will be discussed with descriptions of the pros and cons of each. After weighing these pros and cons and evaluating the assumptions made, the appropriate analysis is chosen for the testing at hand. The subsequent application in a data acquisition and analysis software package is detailed, including modifying the equations for use in the MATLAB language and some of the current drawbacks of the analysis. Conclusions from this work and areas for future work will be discussed to aid future iterations of this analysis.

1. Introduction
The intent of this paper is to allow greater insight into the random errors, or variance, associated with the FRF of an experimentally measured system. While most data acquisition software packages allow varying FRF estimation techniques (H_1, H_2, H_v, etc.) which aim to eliminate bias errors, the variance of the FRF calculation must be reduced using an appropriate number of data ensembles or cyclic averages, if available. However, one cannot always be certain that the number of ensembles acquired has removed the suitable amount of random noise. This is particularly true if the technician is inexperienced or working on a new structure or with new hardware. Therefore, a confidence bounds approach is presented to statistically determine how much of the random noise has been eliminated after a particular number of ensembles for a particular test setup. In addition to giving an indication of the amount of random noise that has been removed, this analysis should be able to provide an actual range wherein the expected FRF will lie.

2. Confidence Bounds Derivation
2.1. Modern Analysis
The analysis more commonly used for the measurement of statistical variance of an FRF comes from a later work of Bendat [3]. According to this analysis, the confidence interval can be defined thusly:

$$\sigma\left(\left|\hat{H}(\omega)\right|\right) = \frac{\sqrt{1-\gamma_{xy}^2(\omega)}}{\gamma_{xy}(\omega)\sqrt{2n_d}}\left|\hat{H}(\omega)\right| \tag{1}$$

Where $\sigma\left(\left|\hat{H}(\omega)\right|\right)$ is the statistical random error, $\gamma_{xy}^2(\omega)$ is the value of coherence at a particular frequency ω, and n_d is the total number of collected data ensembles. For a full explanation of the derivation of this equation, please consult Bendat's later work [3].

Using the above equation to solve for the variance, the FRF confidence bounds can be defined thusly:

$$\left|\hat{H}(\omega)\right| - C_f\sigma\left(\left|\hat{H}(\omega)\right|\right) \leq |H(\omega)| \leq \left|\hat{H}(\omega)\right| + C_f\sigma\left(\left|\hat{H}(\omega)\right|\right) \tag{2}$$

In the above equation, C_f is the Gaussian confidence coefficient for a particular confidence interval, $\left|\hat{H}(\omega)\right|$ is the estimated value of the FRF at a particular frequency ω, and $|H(\omega)|$ is the actual value of the FRF. This equation states that the expected

value of $|H(\omega)|$ will lie between an upper and lower limit of the FRF defined by the calculated FRF and its associated variance. This agrees with comments made earlier in this paper.

This analysis presumes a small error $\sigma\left(\left|\hat{H}(\omega)\right|\right)$<0.10 so that a Gaussian probability distribution can be assumed. However, this assumption is accurate over a very narrow range of measurements, as will be discussed later.

Phase

When the input-output data is collected from the structure multiple measurements are actually calculated using the hardware and software. In the scope of this paper, the phase measurement and its confidence interval is of greatest interest and will be discussed here.

Below is a "confidence diagram" which helps to pictorially describe the confidence interval application to the FRF data collected [2].

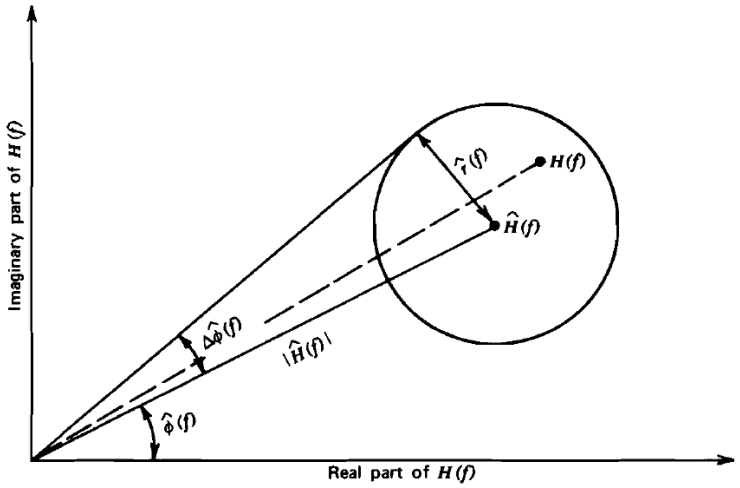

Figure 1 - Confidence Interval Diagram

Inspection of this diagram gives direct insight into how the phase variance can be calculated once the FRF and its confidence interval are determined. From the assumption that the $\sigma\left(\left|\hat{H}(\omega)\right|\right)$ term is small, the small angle theorem applies.

$$\Delta\hat{\phi}(f) = \frac{\sigma(|\hat{H}(\omega)|)}{|\hat{H}(\omega)|} = \frac{\sqrt{1-\gamma_{xy}^2(\omega)}}{\gamma_{xy}(\omega)\sqrt{2n_d}} \tag{3}$$

2.2. Classical Analysis

The equation for the FRF confidence bounds as presented in Bendat's work is presented below. This analysis itself was based on the work of Good man and Enochson [4]. For the exact derivation of this equation, please consult Bendat [2]. This approach makes use of the F-distribution following that the error term is influenced by two statistically independent inputs: the autopower of the input (real and imaginary parts) and the number of ensembles acquired.

$$\sigma\left(\left|\hat{H}(\omega)\right|\right) = \frac{2}{(n_d-2)} F_{2,n_d-2;\alpha}\left[1-\gamma_{xy}^2(\omega)\right]\frac{\hat{G}_{xx}(\omega)}{\hat{G}_{ff}(\omega)} \tag{4}$$

A quick look at this equation reveals that it will not readily work with conventional data acquisition software. This is because of the $\frac{\hat{G}_{xx}(\omega)}{\hat{G}_{ff}(\omega)}$ term. In order to ease integration into the V-Acquisition software, the output power/input power term must be converted to something obtained during an FRF measurement. To get the above Bendat equation into a form that can use these estimators, the following relationships will be used.

$$\frac{\hat{G}_{xx}(\omega)}{\hat{G}_{ff}(\omega)} = \hat{H}(\omega) = \hat{H}_1(\omega) \times \hat{H}_2(\omega) \tag{5}$$

$$\hat{H}_1(\omega) = \frac{\hat{G}_{xf}(\omega)}{\hat{G}_{ff}(\omega)} \tag{6}$$

$$\hat{H}_2(\omega) = \frac{\hat{G}_{xx}(\omega)}{\hat{G}_{xf}(\omega)} \tag{7}$$

$$\gamma_{xy}^2(\omega) = \frac{\hat{H}_1(\omega)}{\hat{H}_2(\omega)} = \frac{\hat{G}_{xf}(\omega)}{\hat{G}_{ff}(\omega)} \times \frac{\hat{G}_{xf}(\omega)}{\hat{G}_{xx}(\omega)} \tag{8}$$

Therefore,

$$\hat{H}(\omega) = \frac{\hat{G}_{xf}(\omega)}{\hat{G}_{ff}(\omega)\times\gamma^2_{xy}(\omega)} = \frac{\hat{H}_1(\omega)}{\gamma^2_{xy}(\omega)} \tag{9}$$

$$\therefore\ \hat{H}(\omega) = \frac{\hat{H}_1(\omega)^2}{\gamma^2_{xy}(\omega)} \quad \text{and} \quad \sigma\left(\left|\hat{H}(\omega)\right|\right) = \sigma\left(\left|\hat{H}_1(\omega)\right|\right) = \frac{2}{(n_d-2)} F_{2,n_d-2;\alpha}\left[1-\gamma^2_{xy}(\omega)\right]\frac{\hat{H}_1(\omega)^2}{\gamma^2_{xy}(\omega)} \tag{10}$$

With this equation the classical Bendat analysis can now use data that is already calculated within data acquisition software. By looking at the above equation, one can come to the conclusion that it only works with the H_1 FRF estimator. This was presented as it is the most common and robust FRF estimator used. Techniques have been devised to potentially evaluate the confidence bounds using other estimators, but that is beyond the scope of this paper.

Phase

Like the more modern analysis, the classical confidence interval analysis makes provisions for measurements other than just the FRF, such as phase. The phase confidence interval is calculated using essentially the same error term as for the FRF itself.

Keeping the $\sigma\left(\left|\hat{H}(\omega)\right|\right)$ term from above the same, the upper and lower limits of the phase can be computed by the following.

$$\Delta\hat{\phi}(\omega) = \sin^{-1}\left[\frac{\sigma(|\hat{H}(\omega)|)}{|\hat{H}(\omega)|}\right] \tag{11}$$

Another look at the confidence diagram shows the validity of the above equation. The $\Delta\hat{\phi}(\omega)$ term represents the angle formed between the measured and calculated FRF and the confidence bounds.

2.3. Old Bendat vs. New Bendat

These two methods will now be compared to see which gives the most way to quantify the variance of the FRF measurement. For this paper, the computational difficulties will be ignored as most can be handled by modern software programs. Below is a table with the error terms as calculated by the classical Bendat analysis [2]. It becomes clear that the assumption of <10% error for the Gaussian distributed technique holds true very little of the time. Furthermore, the terms generated using Bendat's later work are more similar with other published tables than the terms using assuming Gaussian distributed variance [5]. Since this paper aims to find a way of quantifying the random error over a wide range of ensembles and coherence values, the Gaussian method will be discarded.

γ_{xy}^2 / n_d	16	32	64	128	256
0.1	1.22	0.83	0.57	0.40	0.29
0.2	0.81	0.56	0.38	0.27	0.19
0.3	0.62	0.42	0.29	0.21	0.15
0.4	0.50	0.34	0.23	0.16	0.12
0.5	0.41	0.28	0.19	0.13	0.10
0.6	0.33	0.23	0.16	0.11	0.08
0.7	0.27	0.18	0.13	0.09	0.06
0.8	0.20	0.14	0.10	0.07	0.05
0.9	0.14	0.09	0.06	0.04	0.03

Table 1: Classical Bendat Analsysis: Error Terms

2.4. Bias Errors

As has been stated throughout this paper, the usefulness of this analysis is to quantify the *random* error associated with FRF measurements. One can concluded then that it does nothing to address bias errors, particularly leakage as a result of under-sampled data. This is supported by Bendat's assumption that bias errors are negligible for this analysis [2]. However, when the frequency resolution is set too low (large Δf) bias errors will dominate at the resonances and anti-resonances, which may adversely affect the confidence bounds estimates. This is especially true for lightly damped structures where leakage can be a significant factor [1]. For example, the wider, shallower peak resulting from leakage will result in an underestimate value of the upper and lower bounds. In this example, the confidence bounds may not include the actual value of the peak. To correct this, perhaps a different probability distribution should be utilized in these instances.

3. Application in X-Modal III

The initial application of the FRF confidence bounds in a software package was in the X-Modal software package developed by the Structural Dynamics Research Laboratory (SDRL) at the University of Cincinnati. Most commercially available

software packages do not reveal the exact methods used in calculations or assumptions made. This leads to "black box" analyses which don't necessary help ones understanding of the data. Depending on the analysis, this could affect the results and skew the understanding of the structure(s) under analysis. Having direct control allows better understanding of the results of the various tests performed and provides a better learning tool for students. The ability to see exactly how the program is carrying out commands and calculations also make it an ideal test bed for the confidence interval calculations in an actual acquisition and analysis package.

When using the classical Bendat analysis and its associated F-Distribution particular computations must be made. Namely, as the confidence coefficient is dependent on the number of ensembles and number of correlated inputs to a particular FRF (assumed for this case to be one), various tables must be stored and referenced. These tables will provide a value for the confidence coefficient at each Δf [2] [6].

Certain care had to be taken to ensure that the correct values of the FRF and coherence were fed into the analysis. This was accomplished by proper indexing of both the input variables and the confidence bounds values themselves. There also needed to be considerations for different FRF estimators, but this is beyond the scope of this paper.

One issue that could not be resolved was applying the phase confidence intervals to "unwrapped" phase plots. While the equations worked very well in the default "wrapped" display, the unwrapped plots produced messy, unintelligible displays. For this reason, and since the wrapped plots still provide insight into the random variance, this analysis is only applied to the wrapped phase plots.

3.1. Results

For the initial analysis of the Bendat method for confidence bounds, time captured throughput data was used. This allows quicker inspection and debugging of the confidence bounds equation as well as removing all time variance from the analysis. Complete removal of time variance enables different analysis procedures to be used on the same data and the results compared back-to-back. This proved most useful as different iterations of both of Bendat's techniques were investigated throughout the course of this paper.

The test setup will vary through the different parts of this section, but a few general notes will be addressed here. Firstly, the maximum number of ensembles gathered in any single test will be limited to 100. This is primarily a result of the amount of data available for processing using the front-end throughput post-processor. This should not negatively affect the actual results of the analysis as most modal tests are thought to converge at or below 100 ensembles.

For the simulated data, the test setup is as follows:

DSP			**Avg**		**Window**	
Span Freq	800	Hz	Avg Type	RMS w/Cyclic	Window	Hanning - P110
Nr Lines	800		Nr Ensembles	20		
FRF Estimator	H1		Nr Cyclic Blocks per Ensemble	4		
Online FRF	On		Display Update Rate	1		
Pretrigger Delay	0	%	Enable Ensemble Preview	Off		
			Ovld Mode	accept w/ rng		

Table 2: Simulated Data Processing

This is intended to mirror the actual test performed to acquire the data in the first place. As the raw data is already acquired, it is unnecessary to modify the source setup for correct data interpretation.

The first tests were run using an H_1 estimation technique since that is the technique suggested from Bendat's later analysis, although here it will be applied to the classical analysis [3]. While it has been proposed that the FRF estimation technique used may affect the resulting confidence interval, this is beyond the scope of this paper. The final confidence bounds analysis for data processed using the H_1 FRF estimator will be presented first.

Before the results of these tests are presented, there is one important thought worth mentioning. When this analysis was first started, it was hypothesized that the different FRF estimators would yield asymmetric confidence bounds. A quick look at the equations used will show that the FRF will be equally bounded regardless of the estimator used.

The first thing to do is inspect that the measured FRF and phase are in fact bounded by the confidence bounds as calculated by the script. This was checked at various frequencies to see how the script handled noisy data as well as the data at resonances and anti-resonances. Quick examples of the FRF and phase confidence bounds are presented here**.**

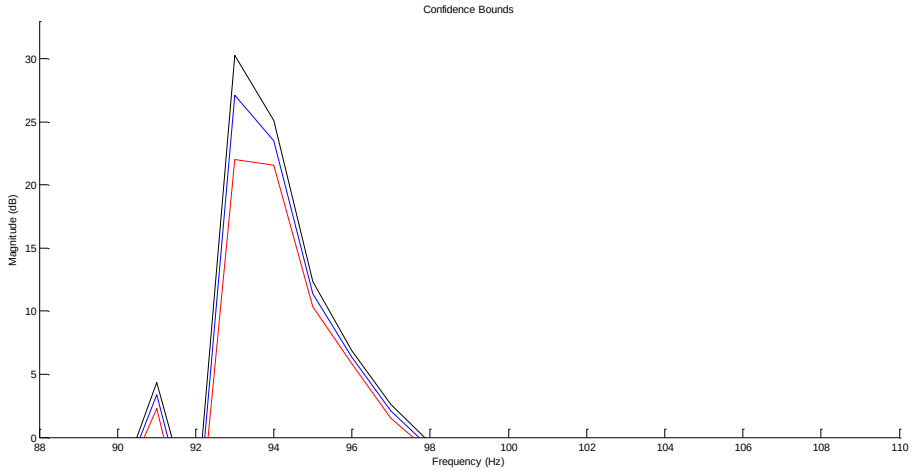

Figure 2 - FRF Confidence Bounds (Close up)

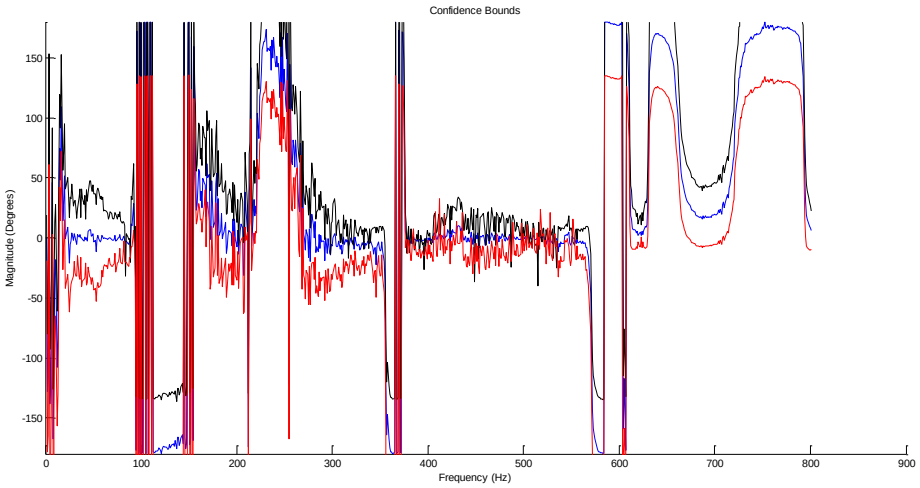

Figure 3 - Phase Confidence Bounds

A quick glance at this data shows what one would expect from the confidence interval calculation. The confidence bounds encapsulate the measured and calculated FRF, with the black line indicating the upper bounds and the red line indicating the lower bounds. The blue line is the plot of the estimate of the actual measured FRF.

This verifies that the script is performing its calculations correctly and shows that the analysis presented herein follows the theory of confidence bounds logically. The applications of this observation will be discussed in greater length in the Conclusions and Future Work section of this thesis.

Next, it is important to verify that both the FRF and phase confidence bounds do in fact become smaller as more and more ensembles are gathered. To do this, a test will be conducted and the resultant FRF and confidence bounds at incremental numbers of ensembles will be saved away. Then, the upper and lower bounds at various frequencies will be inspected at each number of ensembles to see if the bounds are in fact constricting on the measured FRF. Results from this inspection will then be graphed to more easily identify trends in the confidence bounds as a function of ensemble number. This will represent how well the measured data is approaching the expected value as the variance is removed from the data. The plot of these trends is displayed below.

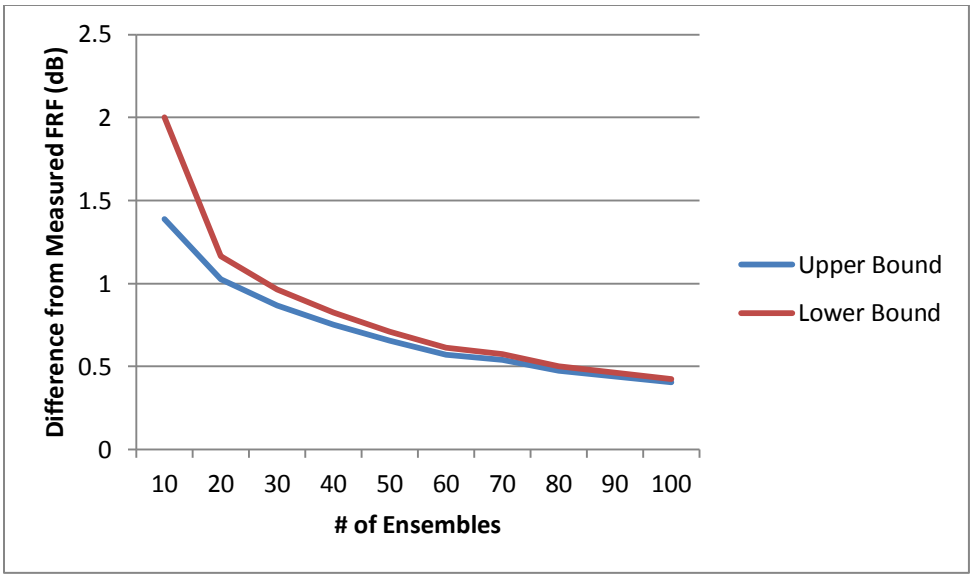

Figure 4 - Confidence Bounds Trend, Test 1 Conditions

The preceding plot does in fact show how the increasing number of ensembles removes variance from the measurement. Of particular note is how the variance drop off is very steep initially and then starts to level out. This is what one would expect from these results: the larger the sample size (number of ensembles in this case), the smaller the variance should become as the error is averaged out in the calculation of the mean FRF.

4. Conclusions and Future Work

The purpose of this paper was to propose a method for quantitatively measuring the random variance present in an FRF measurement. Original methods were presented alongside more contemporary analyses in the attempt to resolve most of the inconsistencies and offer a reasonable and diverse method for FRF confidence bounds analysis. The results of the application of this analysis were then presented to show how the methods presents work with the data.

One possible application of this work in future iterations may include a form of convergence measurement [2]. This can be particularly useful in shaker tests which, while requiring more complicated setups than impact testing, allow the test technician to take an almost unlimited number of ensembles. Of course, this can be limited by the number of data channels, block size, and system memory.

By taking a greater number of ensembles, the technician is able to reduce the amount of variance in the FRF calculation. This will be visibly and numerically illustrated by the confidence bounds. Therefore, an option could be implemented in future software packages where, instead of a user defined number of ensembles, the program itself could determine an acceptable number of averages. The technician could simply setup the hardware and digital signal processing and run the test. When the confidence interval became small enough, as determined either by other experimental data or by user preference, the program would automatically terminate the test. This would help eliminate the need for the technician to pre-select a number of ensembles which may or may not eliminate enough variance.

Furthermore, if the number of ensembles is not enough to sufficiently remove the variance the technician typically would have to start the test all over again. Having a general “convergence” criterion could help eliminate this problem for less experienced technicians. Again, this would work best as an aid. More experienced technicians would likely know the test structure and particular test objectives and, thus, be able to choose a more appropriate number of ensembles.

While most of this analysis is applied in a MIMO setup, it has applications for impact testing and even operational data as well. In impact testing, the confidence bounds analysis can serve as another tool to check the consistency of hammer impacts. When paired with the coherence measurement, this may help reduce the random variance very common in impact testing. In operational data, it can provide the same benefit. Often three or more runs of data are obtained to see which best signifies the operating conditions. Some data acquisition software already compares each run with the average, but this analysis could go one step further. By defining the confidence interval, a technician could see which data runs are actually outliers and discard them from the data. This could help choose data more effectively.

While the idea of applying a confidence interval to an FRF measurement is not a new concept, its use in most data acquisition software is negligible. For this reason, it was applied here to highlight the benefits such an analysis can provide. The potential uses for this technique, particularly the development of a convergence criterion, coupled with its relatively simple integration make it a great new tool for data analysis.

References

1. Allemang, R. J. (2007). *Vibrations: Experimental Modal Analysis.* Cincinnati: UC-SDRL.

2. Bendat, J. S., & Piersol, A. G. (1971). *Random Data: Analysis and Measurement Procedures.* John Wiley & Sons, Inc.

3. Bendat, J. S., & Piersol, A. G. (1993). *Engineering Applications of Correlation and Spectral Analysis: Second Edition.* New York City: John Wiley & Sons, Inc.

4. Enochson, L., & N.R., G. (1965). *Gaussian Approximations to the Distribution of Sample Coherence.* Wright Patterson Air Force Base: Air Force Flight Dynamics Laboratory: Research and Technology Division: Air Force Systems Command.

5. Hewlett Packard. (n.d.). Measuring the Coherence Function with the HP 3582A Spectrum Analyzer. Palo Alto, California, U.S.A: Hewlett Packard.

6. NIST/Sematech. (n.d.). *Upper Critical Values of the F Distribution.* Retrieved May 23, 2011, from Engineering Statistics Handbook: http://www.itl.nist.gov/div898/handbook/eda/section3/eda3673.htm#ONE-10-11-20